ELSEVIER

International Journal of Mass Spectrometry 223–224 (2003) 679–693

International Journal of Mass Spectrometry

www.elsevier.com/locate/ijms

Interpretation of ion distribution functions measured by a combined energy and mass analyzer

K. Ellmer[a], R. Wendt[a], K. Wiesemann[b,*]

[a] *Hahn-Meitner-Institut, Abt. Solare Energetik, Glienicker Straße 100, D-14109 Berlin, Germany*
[b] *Ruhr-Universität Bochum, Experimentalphysik Insbes, Gaselektronik, D-44780 Bochum, Germany*

Received 14 January 2002; accepted 20 June 2002

To the memory of Werner Lindinger, colleague and friend.

Abstract

In plasma chemistry, commercially available systems of combined ion energy and mass analyzers are commonly used for plasma parameter control in processes like plasma supported film deposition or surface modifications. The usual way to measure ion distribution functions by those analyzers is to change the reference potential of the analyzer thereby scanning the distribution function. For interpreting measured ion distribution functions we describe the principle of such a combined ion mass and energy analyzer and calculate the measured ion current and its relation to the ion distribution function. In this way, we show that the measured ion current versus the reference potential of the energy analyzer represents a *velocity* distribution function versus energy. Furthermore, we discuss in how far it is possible to evaluate from this velocity distribution function the total ion current densities and the energy carried by the ions onto a surface exposed to plasma. (Int J Mass Spectrom 223–224 (2003) 679–693)

Keywords: Ion distribution function; Combined ion mass and energy analyzer; Total ion current

1. Introduction

Systems to measure ion distribution functions have found growing interest during the last years. The ion distribution function is considered to be an important parameter for plasma-induced surface modifications [1,2] and for plasma supported thin film deposition [3–5]. Different systems are known for measuring ion distribution functions: time of flight spectrometers [6,7], retarding field analyzers [8,9], and combined energy and mass analyzers [1,2,10–15]. The simplest technique is the retarding field analysis. Here an ion current is measured as a function of a retarding potential. The distribution function is obtained from the derivative of this current with respect to the potential. The dimensions and the ion path lengths inside the analyzer can be made very small. Thus, no differential pumping is required. The whole analyzer can be mounted on a moveable arm to scan large volume plasmas. This technique can be even used in plasmas without external potential reference [16,17]. Its disadvantage is that there is no mass discrimination. The so-called plasma monitor omits this shortcoming. Such systems were already around 1970 described by Coburn [10] and are nowadays commercially available. They consist of a combination of a transverse electric field

* Corresponding author.
E-mail: klaus.wiesemann@ruhr-uni-bochum.de

1387-3806/02/$ – see front matter
PII S1387-3806(02)00940-5

energy analyzer and a mass spectrometer, mostly a quadrupole.

The ion current measured by a plasma monitor is usually displayed versus energy and represents a distribution function. There is some confusion in the literature on the question which kind of distribution function corresponds to this curve. Distribution functions are defined properly in kinetic theory (see, e.g. [18]). The velocity distribution function $f_{\boldsymbol{v}}(\boldsymbol{r}, \boldsymbol{v})$, for example, is the (particle) density in the six-dimensional phase space (three velocity and three configuration space components; Eq. (1)), while the energy distribution function $f_E(\boldsymbol{r}, E_{\text{kin}})$ is the density in a four-dimensional space spanned by one kinetic energy and three configuration space components (Eqs. (23) and (24)). The dependence on the vector $\boldsymbol{r}$ is important, when the potential energy E_{pot} locally varies like in the case considered here.

In many papers, the ion distribution functions measured by plasma monitors are simply named energy distributions [1,2,10–15]. No further explanation is given whether this is justified and how the measured curves relate to the distribution functions defined in kinetic theory. This relation, however, must be known, when comparing results of different measurements or calculating ion densities and the ion fluxes from the measured distribution functions. The aim of this paper is to show what kind of ion distribution function is measured with such a system. Examples for calculating the total ion current and the average ion energy from a measured distribution function are shown in Sections 5.1.3 and 5.1.4, respectively. It is shown that these quantities can be obtained only under very restricted conditions mostly not fulfilled in usual measurements.

2. Plasma monitor

The scheme of a plasma monitoring system is shown in Fig. 1. The whole set is situated in a separately pumped box. Ions enter through a fine hole in the cap. An ion optic, an energy analyzer, a quadrupole for mass selection, and a detector are the four main parts. Typically the energy analyzer is a cylindrical mirror energy analyzer and the detector a secondary electron multiplier detector or a Faraday cup. The ion optic forms an ion beam out of the ions entering the hole in the cap. A part of this beam can pass the energy analyzer and the quadrupole and will finally reach the detector. The formation of an ion beam is accompanied by ion acceleration and deceleration that is a change of the ion potential energy along the ion path. An essential part of this paper is devoted to a consideration

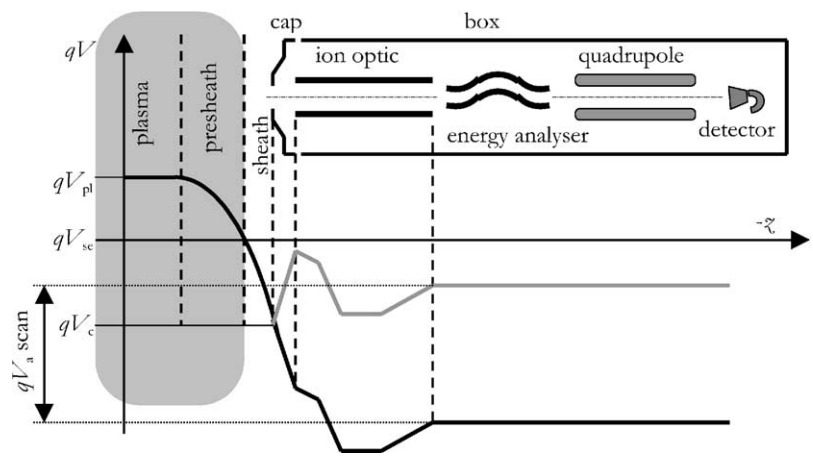

Fig. 1. Scheme of a plasma monitor and typical axial potential course for measuring positive ions: V, electric potential; V_{pl}, plasma potential; V_{se}, potential at the sheath edge; V_c, potential of the cap; V_a, central potential of the energy analyzer.

of the influence of this variation of the potential energy on the measurement of the ion distribution functions.

In general, the distribution function measured can be attributed to that of the ion flux bombarding the cap, which in many cases is the only one of interest. If the plasma monitor is used to investigate the flux of positive ions from a plasma, the cap is in general negatively biased with respect to the plasma and the transition region in front of the cap consists of a space charge sheath and a presheath [19] (see Fig. 1 and Section 3) separating the analyzer from the bulk of the plasma. In case of a collision-free sheath, the according distribution function at the sheath edge can be deduced by considering also the ion acceleration in the sheath. The modification of the distribution function inside the presheath in most cases destroys any information on the ion distribution function inside the bulk plasma. By using a plasma monitor, the bulk plasma distribution function can be obtained only under very special conditions (see discussion below).

For the standard measurement of an ion distribution function, the reference potentials of the ion optic, the cylindrical mirror analyzer, the quadrupole, and of the detector are changed simultaneously. The relative potentials of these components are kept constant during the measurements. The ion current is measured as a function of the reference potential of the energy analyzer and represents the ion distribution function. By multiplying this potential with the charge q of the ions, one gets the energy axis of the distribution function. A plasma monitor in general is suitable to measure positive and also negative ions. To switch from one kind of ions to the other, all potentials inside the plasma monitor and also the voltage across the sheath have to be inverted. The discussion given here applies for both kinds of ions if not otherwise stated.

3. Calculation of the ion current entering a plasma monitor

3.1. General

We restrict ourselves to considering the transformation of the ion distribution function due to acceleration and decelerations in homogenous electric fields without the influence of collisions. This in general holds true for the electric fields in the ion optical system inside the plasma monitor box. It may be valid also in the space charge sheath if that is free of collisions. In that case, our considerations also apply to the sheath. However, the conditions inside the sheath and at its boundary need special discussion. Those inside the plasma monitor are well defined.

As mentioned above, the ionic distribution function at the sheath edge can be evaluated from the measurements, if the space charge sheath in front of the entrance of the plasma monitor is collision free. This distribution function can only be identified with that of the respective ions inside the bulk plasma (or part of it), if no presheath is established between the plasma and the space charge sheath, i.e. only in rather rare cases.

For positive ions there does not exist a presheath if

- the space charge sheath decelerates the ions, i.e. if the entrance diaphragm is more positive than the plasma potential including the limiting case that it is on plasma potential;
- there are no electrons, only negative ions in the plasma (this may happen in afterglows in electronegative gases) [20].

For negative ions there is no presheath, if the space charge sheath accelerates them or they constitute the only negative charge carriers in the plasma.

In all these cases, the distribution function at the sheath edge can be considered to be isotropic.

In the most abundant case of positive ions accelerated to the entrance of the plasma monitor, the distribution function at the sheath edge is established in the presheath. This distribution function is in general highly anisotropic. The ionic flow is a directional flow from the plasma to the sheath edge. However, as the presheath is in most cases collision dominated, there is no way to evaluate from the distribution function at the sheath edge the distribution function inside the bulk of the plasma [21] because the information on the plasma distribution function is almost completely destroyed in the presheath.

If there are collisions (mostly charge exchange) in the space charge sheath, only the (in general anisotropic) distribution function at the entrance of the plasma monitor can be obtained from the measurements. However, this is the distribution function of the ions bombarding a surface exposed to the plasma and for the plasma processes mentioned in the introduction this is mostly the only distribution function of interest. (In case of a collision-free sheath, it is straightforward to obtain this distribution function from that at the sheath edge and vice versa by considering the acceleration in the sheath. This will be discussed later on.)

The density dn of ions at a location $\boldsymbol{r}$ having a velocity in the interval between the vectors $\boldsymbol{v}$ and $\boldsymbol{v} + \mathrm{d}\boldsymbol{v}$ is given by

$$\mathrm{d}n = f_{\boldsymbol{v}}(\boldsymbol{r}, \boldsymbol{v})\mathrm{d}^3 v. \tag{1}$$

Here $\mathrm{d}^3 v$ is the volume element in the velocity space spanned by the three components of the vector $\mathrm{d}\boldsymbol{v}$. The velocity distribution function $f_{\boldsymbol{v}}(\boldsymbol{r}, \boldsymbol{v})$ is in general an explicit function of the components of the velocity $\boldsymbol{v}$. This is symbolized by writing the vector $\boldsymbol{v}$ as the argument. We use as co-ordinates in velocity space the spherical co-ordinates v, φ and θ. Here v is the absolute value of $\boldsymbol{v}$, i.e. the speed of the ions, φ and θ are the Eulerian angles (Fig. 2). In these co-ordinates, we have

$$\mathrm{d}^3 v = v^2 \sin\theta \, \mathrm{d}\theta \, \mathrm{d}\varphi \, \mathrm{d}v \tag{2}$$

and $f_{\boldsymbol{v}}(\boldsymbol{r}, \boldsymbol{v}) = f_{\boldsymbol{v}}(\boldsymbol{r}, v, \theta, \varphi)$. The particle current density $\mathrm{d}\boldsymbol{j}$ of ions having a velocity in the interval between $\boldsymbol{v}$ and $\boldsymbol{v} + \mathrm{d}\boldsymbol{v}$ is given by

$$\mathrm{d}\boldsymbol{j} = \boldsymbol{v}\,\mathrm{d}n = \boldsymbol{v} f_{\boldsymbol{v}}\,\mathrm{d}^3 v = \boldsymbol{v} v^2 f_{\boldsymbol{v}} \sin\theta \, \mathrm{d}\theta \, \mathrm{d}\varphi \, \mathrm{d}v. \tag{3}$$

If an infinitesimal surface element with the normal vector $\mathrm{d}\boldsymbol{A}$ is exposed to the ion flux, the ions with an electric charge q hitting this surface carry an electric current

$$\mathrm{d}(\mathrm{d}I) = q\,\mathrm{d}\boldsymbol{j}\,\mathrm{d}\boldsymbol{A}. \tag{4}$$

The double differential shall symbolize that d(dI) is differential in configuration space as well as in velocity space. In a stationary state, this differential current is constant within the angle of acceptance throughout the entire analyzer while the local distribution functions, current densities, and the particle velocities, respectively the kinetic energies may change according to the changes of the potential energy (even when assuming no collisions to occur along the ion path).

For the sake of simplicity, we assume the ion flux to be homogeneous and the transmission probability to be constant across the area A (which we identify with the entrance of the plasma monitor). Thus, the integration of Eq. (4) across the area A can be replaced by a multiplication with its magnitude A and taking the scalar product of the surface normal vector of A and $\mathrm{d}\boldsymbol{j}$. We choose our co-ordinate system in such a way that $\theta = 0$ corresponds to the direction of the surface normal of A towards the plasma and the angle φ describes a rotation around this surface normal (Fig. 2). Without much loss of generality, we can assume that $f_v(\boldsymbol{r}, \boldsymbol{v})$ does not depend on φ, i.e. $f_{\boldsymbol{v}}(\boldsymbol{r}, \boldsymbol{v}) = f_{\boldsymbol{v}}(\boldsymbol{r}, v, \theta)$. Thus, the φ-integration yields a factor 2π. The θ-integration has to be extended from an angle $\theta_0(v) \geq \pi/2$ to π and we get

$$\mathrm{d}I = 2\pi q A \left\{ \int_{\theta_{0(v)}}^{\pi} \mathrm{d}\theta \cos\theta \sin\theta v^3 f_{\boldsymbol{v}}(\boldsymbol{r}, \boldsymbol{v}) \right\} \mathrm{d}v. \tag{5}$$

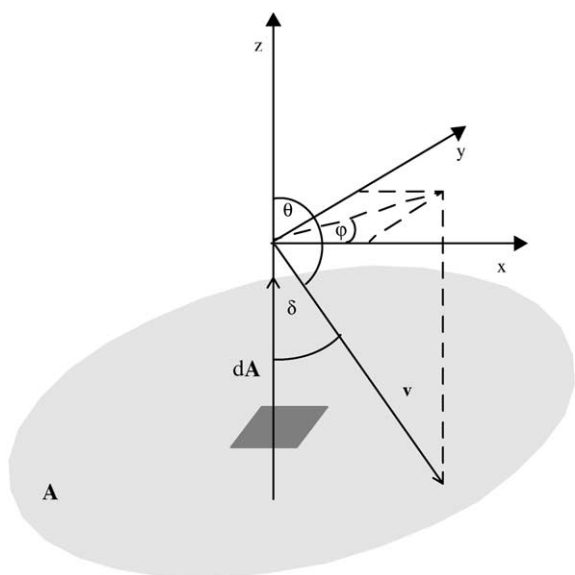

Fig. 2. Relation between cartesian and spherical co-ordinates and definition of $\theta = 0$.

The factor $\cos\theta$ is due to the scalar product of $\mathrm{d}\boldsymbol{j}$ and $\mathrm{d}\boldsymbol{A}$. The angle $\delta(v) = \pi - \theta_0(v)$ is the angular acceptance of the plasma monitor defined by the entrance and exit apertures of the entire ion optical system. Notice that most authors define the angle $2\delta(v)$ as the angle of acceptance (Figs. 4 and 5).

Usually the angle of acceptance of a plasma monitor is very small (of the order of 1° or less [22]), i.e. $\delta(v) \ll \pi$. Therefore, in the evaluation of Eq. (5), we can replace $f_{\boldsymbol{v}}(\boldsymbol{r}, v, \theta)$ by $f_{\boldsymbol{v}}(\boldsymbol{r}, v, \pi)$. Further, Eq. (5) becomes easier to handle if we switch to the angle θ', the velocity v', and the velocity distribution function inside the energy analyzer of the plasma monitor (co-ordinate vector $\boldsymbol{r}_a$), i.e. at the respective potential V_a used for setting for a specific ion group the kinetic energy to ε, the energy, at which ions can pass the energy analyzer. Thus, we obtain

$$\mathrm{d}I = 2\pi qA\left\{\int_{\theta_0'(v')}^{\pi} \mathrm{d}\theta' \cos\theta' \sin\theta' v'^3 f_{\boldsymbol{v}}(\boldsymbol{r}_a, v', \pi)\right\}\mathrm{d}v'. \tag{6}$$

Here $\boldsymbol{r}_a$ is a typical location inside the energy analyzer.

For $\theta = \pi$, we have also $\theta' = \pi$ (acceleration in forward direction). The ion current in general does not change due to the acceleration or deceleration (as long as the acceptance angle is not changed or some ions are repelled). Thus, we do not need to write $\mathrm{d}I$ with a prime in Eq. (6). For small angles, the constancy of the components of the momentum in the directions perpendicular to that of the electric field leads to the following relation between the angles δ and δ'

$$\delta(v) = \delta'(v')\frac{v'}{v}. \tag{7}$$

The θ'-integration in Eq. (6) can be performed and yields for small δ' the factor $-\delta'^2/2$. Thus,

$$\mathrm{d}I = -\delta'^2(v)\pi qAv'^3 f_{\boldsymbol{v}}(\boldsymbol{r}_a, v', \pi)\mathrm{d}v' = qA\,\mathrm{d}j_A \tag{8}$$

is the current of ions through the entrance of the analyzer (with δ' measured in radian). Here $\mathrm{d}j_A$ is the current density of ions with speeds at the entrance of the plasma monitor corresponding to those between v' and $v' + \mathrm{d}v'$. The index 'A' shall indicate that only ions whose velocity vector points into the cone defined by $\pi - \delta' \le \theta \le \pi$ contribute to this current density.

For the integration of Eq. (8), we have to consider the role of the energy analyzer. Its probability of transmission is given by a transmission function $P(\varepsilon, E'_{\mathrm{kin}})$ peaking at ε. Here ε is the nominal kinetic energy to which inside the monitor system the energy analyzer is set. That is the energy the ions must have to pass this analyzer. For example, ions entering the plasma monitor with nearly zero kinetic energy must be accelerated to ε, those entering the analyzer box with an energy larger than ε must be decelerated. The ion current I_D passing the analyzer system and reaching the detector is given by the integral

$$I_D = \int P(\varepsilon, E'_{\mathrm{kin}})\mathrm{d}I. \tag{9}$$

The integration extends over all energies for which $P(\varepsilon, E') \neq 0$. We now get from Eqs. (8) and (9):

$$I_D = -\left(\frac{2\pi qA}{m^2}\right)\int \delta'^2(E'_{\mathrm{kin}})P(\varepsilon, E'_{\mathrm{kin}}) \times E'_{\mathrm{kin}} f_{\boldsymbol{v}}(\boldsymbol{r}_a, E'_{\mathrm{kin}}, \pi)\mathrm{d}E'_{\mathrm{kin}}. \tag{10}$$

Here we have substituted the speed v' by the corresponding kinetic energy $E'_{\mathrm{kin}} = mv'^2/2$. However, $f_{\boldsymbol{v}}$ is still the velocity distribution function, but now it is considered as a function of the kinetic energy. For the further calculation of I_D, we have to distinguish the cases of high and low energy resolution of the energy analyzer.

3.2. High energy resolution

If the energy resolution of the analyzer is sufficiently high for investigating the structure of the distribution function, i.e. if the half-width ΔE of the transmission function $P(\varepsilon, E'_{\mathrm{kin}})$ is small as compared to the half-width of the distribution function, one can neglect the variation of the distribution function over the integration interval and replace it under the integral of Eq. (10) by its value at ε. This usually is the tacitly made assumption when considering a plasma monitor as a means for measuring distribution functions. The same holds true for the angle of acceptance δ' and its

square. Thus, these functions do not depend on the integration variable and we can replace Eq. (10) by

$$I_D = -\left(\frac{2\pi qA\delta'^2(\varepsilon)}{m^2}\right) f_{\boldsymbol{v}}(\boldsymbol{r}_a, \varepsilon, \pi) \times \int P(\varepsilon, E'_{\mathrm{kin}}) E'_{\mathrm{kin}}\, \mathrm{d}E'_{\mathrm{kin}}. \quad (11)$$

This means that the current at the detector of the plasma monitor is proportional to the *forward part of the velocity distribution function* (i.e. at $\theta = \pi$) at the energy defined by the potential settings of the energy analyzer inside the plasma monitor.

The exact shape of the transmission function does not influence the result. We, therefore, can replace the integral over the two-parametric function $P(\varepsilon, E'_{\mathrm{kin}})$ by the product of two parameters, namely the half-width ΔE_ε of the function $P(\varepsilon, E'_{\mathrm{kin}})$ and a transmission P_ε defined by

$$P_\varepsilon \varepsilon \Delta E_\varepsilon =: \int P(\varepsilon, E'_{\mathrm{kin}}) E'_{\mathrm{kin}}\, \mathrm{d}E'_{\mathrm{kin}}. \quad (12)$$

This means that we replace the integrand of Eq. (12) by a rectangle of height $P_\varepsilon \varepsilon$ and width ΔE_ε but with the same area as the integrand. The indices indicate that both parameters may depend on ε. For instance, cylindrical mirror energy analyzers in general have a constant energy resolution $\Gamma = \varepsilon/\Delta E_\varepsilon$ [23]. Using Γ instead of ΔE_ε, we obtain

$$I_D = -\left(2\pi qA\delta'^2(\varepsilon)\frac{P_\varepsilon}{m\Gamma}\right)\varepsilon^2 f_{\boldsymbol{v}}(\boldsymbol{r}_a, \varepsilon, \pi). \quad (13)$$

To get the distribution functions of the ions at the sheath edge or at the entrance of the plasma monitor, we have to replace the distribution function inside the energy analyzer by that valid outside the plasma monitor. Now $f_{\boldsymbol{v}}$ can be expressed as a solution of the collision-free Vlasov-equation as long as collisions are absent. It can be shown by very general considerations that any solution of this equation can be expressed as a sole function of the constants of motion [24]. In case of acceleration or deceleration by an electric field depending only on the space co-ordinate in forward or backward direction (which we assume here) constants of motion are, e.g. the total number of particles, the total energy (i.e. the sum of kinetic and potential energy) and the momentum components perpendicular to the direction of the electric field. For our conclusions, this is a very important property of the velocity distribution functions. To make its implications more clear we consider the simplified case of an isotropic distribution function $f_{\boldsymbol{v}}(\boldsymbol{r}, \boldsymbol{v})$. Isotropic means that $f_{\boldsymbol{v}}$ is an explicit function of v only, not of θ and φ. Thus, in this case

$$f_{\boldsymbol{v}}(\boldsymbol{r}, \boldsymbol{v}) = f_{\boldsymbol{v}}(\boldsymbol{r}, v). \quad (14)$$

The ion potential energy is a unique function of $\boldsymbol{r}$ and the kinetic energy E_{kin} a unique function of v. Without loss of generality, we, therefore, can replace $f_v(\boldsymbol{r}, v)$ by a function $\bar{f}_{\boldsymbol{v}}(E_{\mathrm{pot}}(\boldsymbol{r}), E_{\mathrm{kin}}(v))$. If $\bar{f}_{\boldsymbol{v}}$ can be written as a function of the total energy $E_{\mathrm{tot}} = E_{\mathrm{pot}}(\boldsymbol{r}) + E_{\mathrm{kin}}(v)$, i.e. if

$$\bar{f}_{\boldsymbol{v}}(E_{\mathrm{pot}}(\boldsymbol{r}), E_{\mathrm{kin}}(v)) = \bar{f}_{\boldsymbol{v}}(E_{\mathrm{pot}}(\boldsymbol{r}) + E_{\mathrm{kin}}(v) = E_{\mathrm{tot}}) \quad (15)$$

this means, $\bar{f}_{\boldsymbol{v}}$ does no longer depend on $\boldsymbol{r}$. In case of non-isotropic distribution functions, the situation is more complicated because the functional dependence of $\bar{f}_{\boldsymbol{v}}$ on θ and φ must be considered. We only mention here that for accelerated ions the case of an isotropic distribution function does not simply apply (see Section 5).

For the following, it is important to consider $f_{\boldsymbol{v}}$ as a function of the total energy. Thus

$$f_{\boldsymbol{v}}(\boldsymbol{r}_a, \varepsilon, \pi) = \bar{f}_{\boldsymbol{v}}(\varepsilon + qV_a, \pi). \quad (16)$$

(Eq. (16) must be read as an equation of the *functional value* of $f_{\boldsymbol{v}}$!). Here V_a is the electric potential at which the kinetic energy is equal to ε when the total energy is equal to $(\varepsilon + qV_a)$. The potential V_a may have positive or negative values. Besides, for $\theta = \pi$, Eq. (14) holds for all energies ε and angles φ, respectively, φ' and θ, respectively, θ' for which $f_{\boldsymbol{v}}$ is defined at $\boldsymbol{r}_a$ as well as at $\boldsymbol{r}$ [25]. It is the basic equation for all considerations to follow. There exists no similar equation for the energy distribution function or the distribution function of the absolute values of the velocities (speed distribution function)!

By introducing Eq. (16) into Eq. (13), we see that the current I_D at the detector is a function of ε as well as of the potential V_a:

$$I_D(\varepsilon, V_a) = -\left(2\pi qA\delta'^2(\varepsilon)\frac{P_\varepsilon}{m^2\Gamma}\right) \times \varepsilon^2 \bar{f}_{\boldsymbol{v}}(\varepsilon + qV_a, \pi). \quad (17)$$

A discussion of Eq. (17) is given in Section 4.

3.3. Low energy resolution

If the half-width of the distribution function is small compared to the half-width of the transmission function, we can in reverse neglect the variation of the transmission function $P(\varepsilon, E'_{\text{kin}})$ over the energy range where $f_{\boldsymbol{v}}$ differs from zero, i.e. we can replace $P(\varepsilon, E'_{\text{kin}})$ by its value at $\varepsilon + qV_a$ and the integral in Eq. (10) reduces to

$$I_D(\varepsilon, V_a) = -\left(2\pi q\frac{A}{m^2}\right) P(\varepsilon, \varepsilon + V_a) \times \int f_{\boldsymbol{v}}(\boldsymbol{r}_a, E'_{\text{kin}}, \pi)\delta'^2(\varepsilon)E'_{\text{kin}}\,\mathrm{d}E'_{\text{kin}}. \quad (18)$$

Upon integration, we obtain

$$I_D(\varepsilon, V_a) = j_A qAP(\varepsilon, \varepsilon + V_a) \quad (19)$$

where j_A is the (particle-)current density of ions with velocities pointing into the cone defined by $\pi - \delta \leq \theta \leq \pi$ at the entrance of the plasma monitor. Here ε defines the special setting of the energy analyzer while $\varepsilon + qV_a$ defines the (total) energy of the ions. As mentioned before V_a is varied to scan the ion distribution function. It follows from Eq. (19) that it is possible to measure the transmission function of the analyzer by using an ion beam with a narrow distribution function and varying V_a and the energy of the ion beam. This may be important in case of an ion flux where both P and $f_{\boldsymbol{v}}$ have a half-width of the same order of magnitude. Using an almost mono-energetic ion beam P can be measured and used to deconvolute I_D for $f_{\boldsymbol{v}}(\boldsymbol{r}_a, E'_{\text{kin}}, \pi)$. This, however, will not be further discussed here.

4. Interpretation of the measured ion distribution functions

4.1. General consideration

When replacing V_a by an arbitrary potential $V(\boldsymbol{r})$, Eq. (16) can be used to evaluate at any potential $V(\boldsymbol{r})$, i.e. at any location $\boldsymbol{r}$ in the ion path the velocity distribution function as a function of the kinetic energy by calculating the kinetic energy from the total energy at that potential (as far as collisions are absent) if the minimum kinetic energy of the ions is at V larger or equal to zero. Negative kinetic energies are not defined, $f_{\boldsymbol{v}}(\boldsymbol{r}, E'_{\text{kin}}, \theta) \equiv 0$ for $E'_{\text{kin}} < 0$. Into regions of potential energy, higher than their total energy, ions cannot enter. Thus, from an inspection of the shape of the measured distribution function it is possible to identify the potential at which the distribution function is finally established. It is the potential where $f_{\boldsymbol{v}}$ becomes zero. The uttermost place for which this can be done is at the sheath edge when the sheath is collision free (see discussion above).

If the sheath edge potential is known, say from probe measurements, by this simple criterion the effect of collisions in the space charge sheath can be estimated: The amount of ions having undergone a collision inside the sheath is given by that part of the distribution function with total energies below that corresponding to the sheath edge potential.

At comparatively high pressure, one may measure sometimes distribution functions going to zero at a total energy smaller than the potential energy corresponding to the electric potential of the entrance diaphragm of the analyzer system. This indicates collisions or charge exchange reactions in the unavoidable gas stream entering the analyzer box from the plasma side through the entrance hole. In this case, even the distribution functions of the ions bombarding the plasma-exposed surface of the analyzer entrance can be evaluated only with some error because the distribution functions obtain their final form inside the analyzer box. The magnitude of the according error one can estimate from the part of the measured distribution function at total energies smaller than the potential

energy corresponding to the potential of the entrance cap.

From Eq. (17), we can see the trouble we get in by trying to measure distribution functions by varying the transmission energy ε of the energy analyzer inside the plasma monitor. The angular acceptance and the transmission will change and both have to be known as a function of the transmission energy to evaluate the distribution function from the measured current.

The usual mode of operation of a plasma monitor is to keep ε constant and to vary the reference potential V_a of the analyzer. Then, according to Eq. (17), the measured current is proportional to the *velocity distribution function in forward direction*. This kind of measurement is illustrated in Fig. 3a and b. The ions pass the detector always with the same kinetic energy ε. By changing V_a, the potential of the analyzer, the transmission energy is not changed. What changes is the kinetic energy of the whole ensemble of ions at the analyzer entrance. Thus, for each analyzer potential, the ion current due to a different part of the ion distribution function $f_{\boldsymbol{v}}(\boldsymbol{r}, E'_{\mathrm{kin}}, \pi)$ is measured. In Fig. 3a, the case of ions with an initial energy lower than ε is illustrated. The potential energy at the analyzer qV_{a1} in this case is negative in order to accelerate the ions. In Fig. 3b, we show the case of ions having an initial energy higher than ε. Here the analyzer potential energy qV_{a2} is positive and decelerates the ions. The values of the measured ion distribution function $f_{\boldsymbol{v}}(\boldsymbol{r}_a, E'_{\mathrm{kin}}, \pi)$ represent $f_{\boldsymbol{v}}(\boldsymbol{r}, E'_{\mathrm{kin}}, \pi)$. However, there is a caveat: we assume in our consideration the transmission of the ion optical system to be always the same. Strictly speaking, this transition may depend on the kinetic energy of the ions at the entrance of the plasma monitor and must be taken into account [22].

For calculating quantities like the total ion current or the energy transferred to a plasma-exposed surface, the distribution function $f_{\boldsymbol{v}}(\boldsymbol{r}, E'_{\mathrm{kin}}, \theta')$over the entire velocity space is needed—not only in forward direction that is not only for $\theta = \pi$. We will call $f_{\boldsymbol{v}}(\boldsymbol{r}, E'_{\mathrm{kin}}, \theta')$ the free space distribution function. It can be evaluated from the measured curve only with some additional knowledge on the type of the distribution function. The problem is visualized in Figs. 4 and 5. Here an arbitrarily chosen anisotropic distribution function 1 and its shape 2 after acceleration by a voltage V are shown in a three-dimensional plot. We consider the accelerated function 2 to be $f_{\boldsymbol{v}}(\boldsymbol{r}_a, E'_{\mathrm{kin}}, \theta')$ the one, we would get at $\boldsymbol{r}_a$ if the acceptance angle of the monitor were $\pi/2$, i.e. if all accelerated ions could pass the entire monitor system. However, only that part of $f_{\boldsymbol{v}}(\boldsymbol{r}_a, E'_{\mathrm{kin}}, \theta')$ lying in the cone defined by $\pi - \delta' \leq \theta' \leq \pi$ reaches the final detector. No information on the shape of the distribution function outside this region is contained in the measured curves. Such information, however, is necessary if quantities like the energy deposited by ions on a plasma-exposed surface or the distribution function at the sheath-edge shall be deducted from the

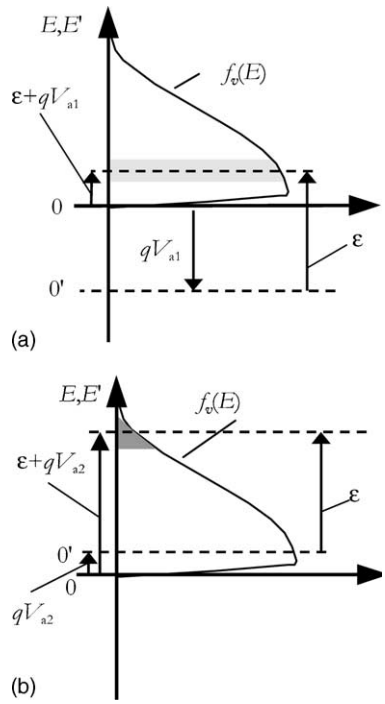

Fig. 3. Illustration of the standard measurement of positive ions with a plasma monitor set to a constant transmission energy ε: E, total energy, respectively, kinetic energy at zero potential energy; the shaded area represents the interval of energies defined by the transmission function $P(\varepsilon, E'_{\mathrm{kin}})$ at which ions can pass the analyzer; $\varepsilon + qV_{\mathrm{ai}}$, mean total energies of those ions; 0, zero of total energy E, 0′, zero of kinetic energy E' for ions at the potentials V_{ai}. (a) Ions are accelerated to pass the energy analyzer (see potential curves in Fig. 1); (b) ions are decelerated to pass the energy analyzer.

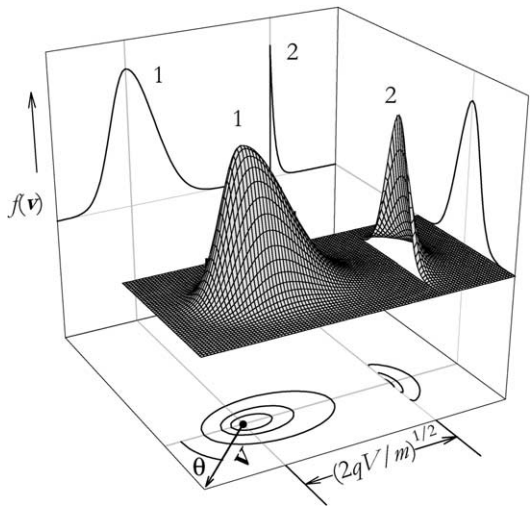

Fig. 4. Three-dimensional plot of an anisotropic velocity distribution function 1 before and 2 after acceleration by a voltage V over the half-planes $\varphi = 0$ and $\varphi = \pi$. Two-dimensional plots obtained by parallel projections are shown on the backside and front walls of the co-ordinate system. At the bottom, a contour plot is given.

measured distribution function. This information can be only obtained by a more or less educated guess or by carefully analysing the fate of the ions inside the presheath and the sheath.

An interesting feature of accelerated distribution functions in velocity space can be seen in Fig. 4 on the two-dimensional parallel projection of the distribution function to the back wall: in velocity space the accelerated distribution function is much narrower than the original one. This effect is very well known and used for the reduction of the Doppler-width of spectral lines in optical spectroscopy [27,28]and for beam cooling by accelerated electrons in accelerator physics.

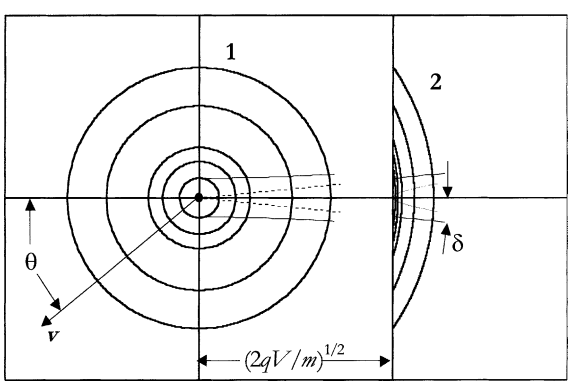

Fig. 5. Contour plot of an isotropic velocity distribution function 1 before and 2 after acceleration by V. The thin straight lines limit that part of the distribution function that can enter an acceptance angle δ of 100 mrad. The full lines are for the case that for the *accelerated* particles the acceptance angle is independent of the velocity; dotted lines are for the case that *before acceleration* the acceptance angle is independent of velocity.

5. Evaluation of free space distribution functions

5.1. Isotropic free space distribution functions

5.1.1. Some general remarks

Up to now, we have developed an expression for the ion current measured by a plasma monitor. The current is proportional to that part of the velocity distribution function that passes the monitor and reaches the detector. As the acceptance angle is very small, one measures only the velocity distribution function in forward direction. However, what is needed is the entire free space distribution function of those ions that bombard the entrance diaphragm or more generally a plasma-exposed surface. To construct it from the measured part of the distribution function, we need additional information. The simplest case would be if we know that the free space distribution function is isotropic where the acceleration starts. At the entrance of the plasma monitor, an almost isotropic distribution function can never exist if the entrance diaphragm is biased. However, at the sheath edge such a distribution function may exist if there is no presheath (see discussion in Section 3). This situation can be analysed simply only if the sheath is collision free. This case can be identified from the conditions of the plasma and the shape of the measured distribution function. That should consist of a single very sharp peak that has a half-width small as compared to the electron temperature (which of course must be known). This rather rare case we will take as a model case because we can give an unambiguous reconstruction recipe for the free space distribution function—not only at the sheath edge but also at the entrance of the monitor. This shall

serve as a model case for the more difficult (and more significant) general case of an unknown anisotropic ion distribution function in the ion flux bombarding the entrance diaphragm.

5.1.2. Reconstruction of the free space distribution function

We consider ions accelerated from an isotropic free space distribution function at zero potential energy by a dc-potential V_a across the sheath and/or inside the analyzer box towards the energy analyzer. The situation before and after acceleration is shown as a contour plot in Fig. 5. Only half of the free space distribution function 1 is accelerated, i.e. that part of it that is constituted by ions having a non-zero velocity component in the direction $\theta = \pi$. This corresponds to the angular range $\pi/2 < \theta \leq \pi$. Accelerated ions never obey an isotropic distribution function—even before acceleration. The contour plot of the distribution function of the accelerated ions like that of the free space distribution function consists of spheres concentric around the point $v = 0$. The distribution function of the accelerated ions can again be considered as part of an isotropic distribution function. This can be understood as follows: before acceleration in velocity space, the points representing ions with the same kinetic energy E_{kin1} are all situated on a spherical half shell defined by $v = (2E_{\mathrm{kin1}}/m)^{1/2}$, $\pi \geq \theta \geq \pi/2$. After acceleration by a voltage V_a, all these ions again have the same kinetic energy namely $E_{\mathrm{kin1}} + qV_a$. The points representing them again are situated on part of a spherical shell defined by $v = (2[E_{\mathrm{kin1}} + qV_a]/m)^{1/2}$, $\pi \geq \theta \geq \arccos(-[E_{\mathrm{kin1}} + qV_a]^{-1/2})$. This is shown in Fig. 5. The anisotropy of the accelerated distribution function comes only from the fact that a well-defined part of the velocity space is empty. The shape of the *velocity* distribution function versus total energy, $\bar{f}_{\boldsymbol{v}}$, does not change when it is accelerated (Eq. (16)). This was demonstrated in Fig. 3: distribution functions at different locations with different potential energy differ only by the zero points of the energy scales. Thus, $\bar{f}_{\boldsymbol{v}}$ can be reconstructed at any potential if only its value for $\theta = \pi$ is known.

According to the energy principle, there is after acceleration no ion with a velocity v' having in the direction $\theta' = \pi$ a component smaller than $(2qV/m)^{1/2}$. If δ' is the angle of acceptance of the analyzer system only that part of the accelerated distribution function within a cone with the angle δ' is finally measured. The cross section of this cone in the half-planes $\varphi = 0$ and $\varphi = \pi$ of the velocity space is shown in Fig. 5 for the case $\delta' = 100$ mrad. We have chosen this comparatively large angel of acceptance to make clearer all phenomena occurring. In usual commercial systems, δ' is of the order of 10 mrad or less and the approximations used in the previous section apply.

A more rigorous treatment has to integrate the distribution function over the angle θ' from $\pi - \delta'$ to π to obtain the measured distribution function. This yields a factor $(1 - \cos\delta')$ if $f_{\boldsymbol{v}}$ is isotropic over this range. However, for velocities v' having an absolute value smaller than $(2qV/m)^{1/2}/\cos\delta'$ the lower limit of integration has to be replaced by $\pi - \theta'_g$, where $\cos\theta'_g = (2qV/mv'^2)^{1/2}$. This is due to the fact that the distribution function of the accelerated ions is limited to the range $\pi - \theta'_g \leq \theta' \leq \pi$ (see [25] for details). Thus, the integration yields over the velocity range $(2qV/m)^{1/2} \leq |v'| \leq (2qV/m)^{1/2}/\cos\delta'$, the velocity and acceleration voltage dependent factor $\{1 - (2qV/mv'^2)^{1/2}\}$ forcing the measured function to go to zero at $mv'^2/2 = qV$. If δ' is sufficiently small this effects only a slight smoothing of the low energy shoulder of the measured distribution function, which can be neglected because the smoothing by the finite energy resolution of the energy analyzer is in general much more effective. Even in the case shown in Fig. 5, with $\delta' = 100$ mrad, the influence of this effect on the measured distribution function is negligibly small as $1/\cos(100\,\mathrm{mrad}) = 1.005$. (If, however, the angular acceptance of the system becomes of the order of $\pi/2$ this effect has to be taken into account.) In the case considered here, the measured distribution function represents in good approximation the velocity distribution function in forward direction which for an isotropic distribution function in free space represents the velocity distribution function over the entire velocity space (as far as it is occupied).

5.1.3. Total ion current

In the case of an isotropic free space distribution function, it is easy to calculate from the measured distribution function the total ion current and the average and total ion energy at the surface behind which the measurements are performed because we can simply make a transformation of the distribution function back to the starting place where it is isotropic, i.e. integrate over $f_{\boldsymbol{v}}(\boldsymbol{r}, v)$instead of over $f_{\boldsymbol{v}}(\boldsymbol{r}_a, v')$.

For calculating the total ion (particle) current density j of ions with the mass m onto a surface at the potential V_c we have to integrate dj over one-half of the velocity space, which means that the θ integration extends over the range $\pi/2 < \theta \leq \pi$ with the limits of the other integrations unchanged. This θ integration is very simple because $f_{\boldsymbol{v}}$ does not depend on θ. Thus, the absolute value of the current density j is given by

$$\mathrm{d}j = 2\pi \int_{\pi/2}^{\pi} \mathrm{d}\theta \cos\theta \sin\theta v^3 f_{\boldsymbol{v}}(\boldsymbol{r}, v)\, \mathrm{d}v. \tag{20}$$

Substituting v by the kinetic energy $mv^2/2$ and replacing $f_{\boldsymbol{v}}$ by $\bar{f}_{\boldsymbol{v}}$ and integrating over θ and V_a (ε is constant) yields:

$$j = \frac{2\pi}{m^2} \int_{qV_a=-\varepsilon}^{qV_a=\infty} (\varepsilon + qV_a)\, \bar{f}_{\boldsymbol{v}}(\varepsilon + qV_a) \mathrm{d}(qV_a). \tag{21}$$

With Eq. (17) now

$$j = \frac{\Gamma}{Aq\delta'^2 P_\varepsilon \varepsilon^2} \int_{qV_a=-\varepsilon}^{qV_a=\infty} (\varepsilon + qV_a) I_D(\varepsilon, V_a) \mathrm{d}(qV_a). \tag{22}$$

Here the zero of V_a is defined in such a way that the original isotropic free space distribution function occurs at a space potential equal to $-\varepsilon/q$. That means the potential at which the free space isotropic distribution function occurs is defined as the zero of the potential energy. (If one wants to define the zero potential energy in a different way, e.g. by the potential of a grounded electrode, an according linear transformation of the energy scale is necessary.) Eq. (22) is suitable to calculate the ion current onto a surface having a potential energy equal to or lower than that corresponding to the plasma potential V_{pl}. If the potential energy at the surface is more positive than the plasma potential energy qV_{pl}, the sheath retards ions and the calculation is not valid any more because it does not consider slow ion reflection at regions of positive potential energy.

5.1.4. Mean and total ion energy

The mean kinetic energy $\langle E \rangle$ of ions arriving at a surface at a potential V_c can be expressed by

$$\langle E \rangle = \frac{\int_{j(E=0)}^{j(E=\infty)} E_{\mathrm{kin}}(V_c) \mathrm{d}j}{\int_{j(E=0)}^{j(E=\infty)} \mathrm{d}j}. \tag{23}$$

Here $E_{\mathrm{kin}}(V_c)$ is the ion kinetic energy at the potential V_c. It is given by

$$E_{\mathrm{kin}}(V_c) = \varepsilon + q(V_a - V_c).$$

Thus, according to Eqs. (18)–(20), the mean kinetic energy $\langle E \rangle$ is given by

$$\langle E \rangle = \frac{\int_{qV_a=-\varepsilon}^{qV_a=\infty} (\varepsilon + qV_a - qV_c)(\varepsilon + qV_a) I_D(\varepsilon, V_a) \mathrm{d}(qV_a)}{\int_{qV_a=-\varepsilon}^{qV_a=\infty} (\varepsilon + qV_a) I_D(\varepsilon, V_a) \mathrm{d}(qV_a)}. \tag{24}$$

It is sometimes claimed that the center of gravity of the area below the measured curve gives the mean energy. From Eq. (24), it is obvious that this is not correct. An example is given in Fig. 6. Whereas the center of gravity is at 16.5 eV the mean energy is $\langle E \rangle = 20$ eV at zero potential energy. For strongly accelerated ions, this difference may be small if the common energy is small as compared to the energy spread described by the distribution function. The total energy flux due to the ion current to a surface at a potential V_c is given by the kinetic energy times the total ion current and therefore proportional to the numerator in Eq. (24).

5.2. Anisotropic free space distribution functions

A typical example of an anisotropic distribution function is that of the positive ions at the edge of a space charge sheath. These ions' distribution function has been changed in the presheath and is in general highly anisotropic. It may have some similarity to that

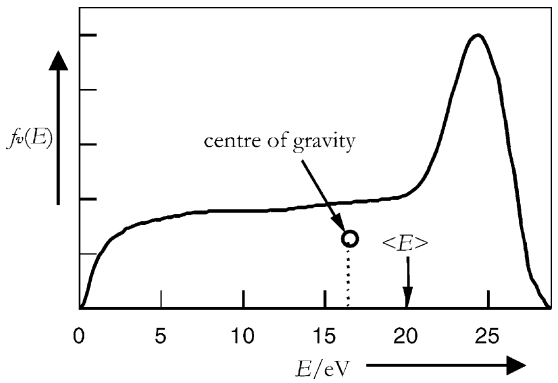

Fig. 6. Typical shape of ion distribution functions measured at a negatively biased wall [8,9,26]. Indicated in the figure are the center of gravity at 16.5 eV and the mean energy of the ions $\langle E \rangle$ at 20 eV calculated by assuming an isotropic free space distribution function.

of a drifting ion swarm [29]. The anisotropy increases further in the space charge sheath.

The distribution function measured is the velocity distribution function in forward direction as in the case of isotropic distribution functions. If there are no collisions in the space charge sheath, it is possible by using $\bar{f}_v$ to trace back from the measured function to the distribution function in forward direction at the sheath edge if the potential at this location is known as described in the previous section. In any other case, only the distribution function at the entrance of the plasma monitor system, i.e. the distribution function of the ions bombarding the entrance diaphragm and any surface having the same potential can be obtained from the measured distribution function. However, as long as there is no additional information on the type of anisotropy of the distribution function, it is impossible to reconstruct the entire free space distribution function from the measured curves. Thus, it is in general not possible to calculate quantities like the total ion current (which may be used for calculating the plasma density) or the average ion energy. Even the energy distribution function cannot exactly be obtained from the measurements because information on the energy content of the degrees of freedom for movement in the directions perpendicular to the direction $\theta = \pi$ are missing. If the space charge sheath is not collision free, experiments and computer simulations have shown that this energy cannot be neglected [29,30]. It comes from scattering of the ion momentum in elastic and charge transfer collisions. The sometimes-heard opinion that charge exchange reactions occur without momentum transfer between the colliding particles is not exactly true [31,32]. Jane and Huth for instance [22] found angular ion distributions having for distinct energies in the range of 100–300 eV, a minimum in forward direction and peaking around $\pm 1^\circ$. In an inductively coupled plasma, Woodworth et al. [33] found behind a collision-free sheath angular distributions with a half-width between 6 and 7.5° i.e., about six times broader than the acceptance angle of a typical plasma monitor. Modelling the effects of collisions and charge exchange reactions inside the sheath on the ion angular distributions Kushner found for the case of a capacitively coupled discharge angular distributions with half-width of the order of 5–8°. The half-width increased with increasing pressure; however, the angular distributions peaked at 0° [34]. Several other authors found similar results [35–37]. The effect of elastic collisions turned out to be a reduction of the number of ions arriving at normal incidence. These examples show that the ion angular distributions though very anisotropic and peaking in forward direction are much broader than the acceptance angle of a plasma monitor.

Thus, an unambiguous evaluation of the energy distribution function of the ions is not possible except one measures the angular variation of the distribution function by a tiltable analyzer as Janes and Huth did [22]. The same holds true also for calculating mean values like the average energy transport from a plasma to a wall. In case of only few collisions in the space charge sheath, one may much more reliably estimate the energy transport by simply taking the product of the total electric current to the wall and the sheath voltage (if that is known). This estimate takes into account both the energy transport by ions and that by fast neutrals produced in charge exchange reactions. For a determination of the energy transport to a substrate measured by the temperature change at the substrate in a magnetron-sputtering device see [38].

6. Conclusions

Compared to a measurement by varying ε measuring ion distribution functions with a plasma monitor by varying V_a has the advantage that the transmission function of the analyzer is independent of the ion energy in the original distribution. The transmission of the ion optical system may change when changing V_a; however, these changes can be made small if the optical system is constructed according to the state of the art [39,40].

Following our calculation, the ion velocity distribution in forward direction and not the energy distribution function is measured by varying V_a. The same kind of distribution functions is measured with a retarding field analyzer [8,9]. For different discharges [1,2,10–15], the velocity and not the energy distribution function have been published. The relation between energy distribution function $f_E(\boldsymbol{r}, E)$ and velocity distribution function $f_{\boldsymbol{v}}(\boldsymbol{r}, [2E_{\mathrm{kin}}/m]^{1/2}, \varphi, \theta)$ is:

$$f_E(\boldsymbol{r}, E_{\mathrm{kin}}) = \left(\frac{2E_{\mathrm{kin}}}{m^3}\right)^{1/2} \int_0^{2\pi} \mathrm{d}\varphi \int_0^{\pi} \mathrm{d}\theta \sin(\theta) \times f_{\boldsymbol{v}}\left(\boldsymbol{r}, \sqrt{\frac{2E_{\mathrm{kin}}}{m}}, \varphi, \theta\right). \quad (25)$$

Here E_{kin} is the kinetic energy at zero potential energy. In case of an isotropic distribution function, i.e. if $f_{\boldsymbol{v}}(\boldsymbol{r}, \boldsymbol{v}) = f_{\boldsymbol{v}}(\boldsymbol{r}, v)$, the integration over the angles can be performed and yields a factor 4π. Thus, Eq. (25) reduces to

$$f_E(\boldsymbol{r}, E_{\mathrm{kin}}) = 4\pi \left(\frac{2E_{\mathrm{kin}}}{m^3}\right)^{1/2} f_{\boldsymbol{v}}\left(\boldsymbol{r}, \left[\frac{2E_{\mathrm{kin}}}{m}\right]^{1/2}\right). \quad (26)$$

As an example in Fig. 7, the energy distribution function corresponding to the velocity distribution function of Fig. 6 is shown assuming that the original velocity distribution function is isotropic in velocity space. Notice that the shape (Fig. 6) and the absolute values (Eq. (26)) are different for both types of distribution functions.

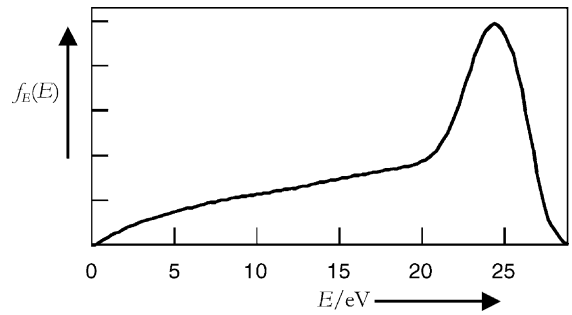

Fig. 7. Energy distribution function corresponding to the curve shown in Fig. 6 assuming an initially isotropic free space distribution function (Eq. (26)).

In conclusion, plasma monitors described in this paper do not measure the ion energy distribution function directly. Due to their small acceptance angle, practically the velocity distribution function in forward direction is measured. In case of isotropic distribution functions, the relation between velocity and energy distribution functions looks comparatively simple. This relation would be similarly simple for anisotropic distribution functions if the integral over a solid angle of 2π could be directly measured. This would be the case if the acceptance angle of the monitor were $\delta = \pi/2$ and the energy analyzer sensitive to the entire kinetic energy of an ion, not only to the kinetic energy due to only one velocity component (as in the case of a retarding field analyzer). However, even in these cases the reliability of calculating the energy distribution function depends on the error in determining the zero of the kinetic energy.

Due to the influence of a presheath on the ion distribution functions, the case of an isotropic free space distribution function is very rare. We are not aware of any general recipe for determining from the forward part of an anisotropic distribution function the complete free space distribution function—even at the surface of a plasma-exposed wall. Obviously, there is a need for an at least two-dimensional kinetic theory of the ion velocity distribution function in a presheath and in a collision dominated space charge sheath.

Our considerations are based on a formulation of the velocity distribution function in spherical

co-ordinates. This comparatively easily leads to Eq. (16), which makes a transformation of the distribution function from one place to the other very simple. The same does not hold true if the distribution function is formulated in cartesian co-ordinates and a one-dimensional energy distribution is defined by neglecting the energy stored in momentum components perpendicular to the direction of acceleration (see [41,42]). As usual plasma monitors do not measure the part neglected, it is difficult to get an estimate of the error inherent in this definition. Nevertheless, this type of distribution function may be an approximation, valid as long as the energy gained by acceleration is large as compared to the energy stored in the momenta perpendicular to the direction of acceleration. However, the expression for this one-dimensional energy distribution function is very different from the generally accepted one given in Eqs. (25) and (26). To our knowledge, the relation between these different expressions has not been given and it is not clear to us. It seems to us that great caution is necessary when using this type of distribution function especially when transforming the distribution function to positions with higher potential energy.

Acknowledgements

We are grateful to K.-U. Riemann for discussions and valuable hints and to D. Meyer for critically reading the manuscript.

References

[1] F. Becker, I.W. Rangelow, R. Kassing, J. Appl. Phys. 80 (1996) 56.
[2] R.J.M.M. Snijkers, M.J.M. van Sambeek, M.B. Hoppenbrouwers, G.M.W. Kroesen, F.J. de Hoog, J. Appl. Phys. 79 (1996) 8982.
[3] J. Robertson, Diamond Rel. Mat. 2 (1993) 984.
[4] S. Reinke, M. Kuhr, W. Kulisch, R. Kassing, Diamond Rel. Mat. 4 (1995) 272.
[5] F. Richter, Physikalische Blätter 52 (1996) 355 (in German).
[6] K. Tominaga, S. Iwamura, Y. Shintani, O. Tada, Jpn. J. Appl. Phys. 21 (1982) 688.
[7] K. Schäfer, W.Y. Baek, K. Förster, D. Gassen, W. Neuwirth, Z. Phys. D: Atoms, Molecules and Clusters 21 (1991) 137.
[8] K.-U. Riemann, U. Ehlemann, K. Wiesemann, J. Phys. D: Appl. Phys. 25 (1992) 620.
[9] U. Flender, K. Wiesemann, J. Phys. D: Appl. Phys. 27 (1994) 509; Erratum ibid. 27 (1994) 1579.
[10] W. Coburn, Rev. Sci. Instrum. 41 (1970) 1219.
[11] J.P. Krumme, R.A.A. Hack, I.J.M.M. Raaijmakers, J. Appl. Phys. 70 (1991) 6743.
[12] J.K. Olthoff, R.J. Van Brunt, S.B. Radovanov, Appl. Phys. Lett. 67 (1995) 473.
[13] J.K. Olthoff, R.J. Van Brunt, S.B. Radovanov, J. Appl. Phys. 72 (1992) 4566.
[14] K. Sando, M. Sugawara, Jpn. J. Appl. Phys. 35 (1996) L171.
[15] M. Zeuner, H. Neumann, J. Meichsner, J. Appl. Phys. 81 (1997) 2985.
[16] A.-M. Pointu, E. Stamate, K. Wiesemann, in: K. Tachibana, Y. Watanabe (Eds.), Proceedings of the Third International Conference Reactive Plasmas and Fourteenth Symposia Plasma Process, Nara, Japan, 1997, Jpn. Soc. Appl. Phys. (1997) 243.
[17] A.-M. Pointu, E. Stamate, K. Wiesemann, Czech. J. Phys. 48 (1998) 1147.
[18] H. Vogel, Gehrtsen Physik, 18th Edition, Springer, Heidelberg, Berlin, 1995, p. 225 (in German).
[19] K.-U. Riemann, J. Phys. D: Appl. Phys. 24 (1991) 493.
[20] H. Amemiya, J. Phys. Soc. Jpn. 67 (1998) 1955.
[21] S. Bieler, G. Ecker, K.-U. Riemann, Phys. Fluids 31 (1988) 1999.
[22] J. Janes, Ch. Huth, J. Vac. Sci. Technol. A 10 (1992) 3522.
[23] A. Barrie, in: D. Briggs (Ed.), Handbook of X-ray and Ultraviolet Photoelectron Spectroscopy, Heyden, London, 1978, p. 79.
[24] G. Ecker, Theory of Fully Ionized Plasmas, Academic Press, New York and London, 1972, p. 95.
[25] K. Wiesemann, J. Phys. E: Sci. Instrum. 14 (1981) 1404.
[26] J.G. Séguin, C.H. Dugan, J.M. Goodings, Int. J. Mass Spectrom. Ion Phys. 9 (1972) 203.
[27] W.H. Wing, G.A. Rutt, W.E. Lamb, J.J. Spezeski, Phys. Rev. Lett. 36 (1976) 1488.
[28] S.L. Kaufman, Opt. Commun. 17 (1976) 309.
[29] H.R. Skullerud, S. Holmstrom, J. Phys. D: Appl. Phys. 18 (1985) 2375.
[30] J. Liu, G.L. Huppert, H.H. Sawin, J. Appl. Phys. 68 (1990) 3916.
[31] B. Huber, Z. Physik. A 275 (1975) 95.
[32] B.A. Huber, H.J. Kahlert, J. Phys. B: Atom Mol. Phys. 13 (1980) L159.
[33] J.R. Woodworth, M.E. Riley, P.A. Miller, G.A. Hebner, J. Appl. Phys. 81 (1997) 5950.
[34] M.J. Kushner, J. Appl. Phys. 58 (1985) 4024.
[35] D. Field, D.F. Klemperer, P.W. May, Y.P. Song, J. Appl. Phys. 70 (1991) 82.
[36] P.W. May, D. Field, D.F. Klemperer, J. Appl. Phys. 71 (1992) 3721.
[37] B.E. Thompson, H.H. Sawin, J. Appl. Phys. 63 (1988) 2241.
[38] R. Wendt, K. Ellmer, K. Wiesemann, J. Appl. Phys. 82 (1997) 2115.

[39] H.-J. Kahlert, Hochauflösende Translationsspektroskopie zur Untersuchung von Elektronentransfer- und Transferionisationsprozessen beim Stoß von Ne^{2+}- und Ar^{3+}-Ionen mit Edelgasatomen, Dissertation, Ruhr-Universität Bochum, 1983 (in German).
[40] E. Harting, F.H. Read, Electrostatic Lenses, Elsevier, Amsterdam, Oxford, New York, 1976.
[41] J.E. Allen, J. Phys. D: Appl. Phys. 25 (1992) 1839.
[42] M.V.V.S. Rao, R.J. Van Brunt, J.K. Olthoff, Phys. Rev. E 54 (1996) 5641.